Size-Focusing Synthesis, Optical and Electrochemical Properties of Monodisperse $Au_{38}(SC_2H_4Ph)_{24}$ Nanoclusters

Huifeng Qian, Yan Zhu, and Rongchao Jin*

Department of Chemistry, Carnegie Mellon University, Pittsburgh, Pennsylvania 15213

ABSTRACT We report a facile, high yielding synthetic method for preparing truly monodisperse $Au_{38}(SC_2H_4Ph)_{24}$ nanoclusters. The synthetic approach involves two main steps: first, glutathionate (−SG) protected polydisperse Au_n clusters (n ranging from 38 to ~102) are synthesized by reducing Au(I)−SG in acetone; subsequently, the size-mixed Au_n clusters react with excess phenylethylthiol (PhC_2H_4SH) for ~40 h at 80 °C, which leads to $Au_{38}(SC_2H_4Ph)_{24}$ clusters of molecular purity. Detailed studies by mass spectrometry and UV−vis spectroscopy explicitly show a gradual size-focusing process occurred in the thermal etching-induced growth process. The formula and molecular purity of $Au_{38}(SC_2H_4Ph)_{24}$ clusters are confirmed by electrospray ionization (ESI) and matrix-assisted laser desorption ionization (MALDI) mass spectrometry, and size-exclusion chromatography. The optical and electrochemical properties of $Au_{38}(SC_2H_4Ph)_{24}$ clusters show molecule-like behavior and the HOMO−LUMO gap of the cluster was determined to be ~0.9 eV. The size focusing growth process is particularly interesting and may be exploited to synthesize other robust gold thiolate clusters.

KEYWORDS: gold clusters · Au_{38} · thiolate · monodispersity · stability

Quantum-sized metal nanoparticles, also called nanoclusters (or clusters for short), have become one of the important types of nanomaterials being extensively pursued in current nanoscience research.[1−3] Metal nanoclusters often undergo drastic changes in the atomic packing structure when the particle size is shrunk to the ultrasmall size regime (typically <2 nm); this is in contrast with semiconductor clusters whose atomic packing structure is typically similar to that of semiconductor nanocrystals.[4] This distinct difference is partly caused by a strong quantum confinement effect in metal nanoclusters[5] and also by the fundamental differences in the nature of the electronic structure between metals and semiconductors.

Although some theoretical work had been done long before on the prediction of the electronic structure of quantum-sized metal nanoparticles, experimental work has long been hampered by the unavailability of well-defined metal nanocluster systems for in-depth studies, and current understanding on the optical and electronic properties of metal nanoclusters (*e.g.*, Au and Ag) is still quite limited. Another major issue in the research of metal nanoclusters is the need to solve their crystal structures since the cluster's electronic and optical properties are structure sensitive or highly dependent on their atomic packing structures.[5] A prerequisite to structure determination of nanoclusters is to grow high quality single crystals for X-ray diffraction analysis; this, however, has long been difficult due primarily to the insufficient monodispersity of metal nanoclusters in most syntheses. Therefore, it is of paramount importance to develop synthetic chemistry that permits the synthesis of monodisperse nanoclusters if the full potential of this new type of nanomaterial is to be realized.

Among noble metals, gold nanoclusters have received particular research interest due to their chemical stability and elegant optical properties, and tremendous work has been done in the past decade.[6−20] It is quite surprising to realize that even after more than a century's intense research on gold nanoparticles since Faraday's time (~1850s),[21] the size-dependent properties of gold nanoparticles are still not fully understood to date, especially in the ultrasmall size regime (<2 nm). The scientific research on gold nanoparticles will apparently last longer. For chemists, one of the major tasks is to develop synthetic strategies for preparing monodisperse Au_n nanoclusters with control over size and structure, and ultimately to understand and utilize the material properties of these clusters for practical applications.[22−25] Unlike gas phase (bare) gold clusters,[26,27]

*Address correspondence to rongchao@andrew.cmu.edu.

Received for review September 1, 2009 and accepted October 18, 2009.

Published online October 27, 2009.
10.1021/nn901137h CCC: $40.75

solution phase clusters need to be protected by appropriate ligands. Since the mid-1990s, stimulated by the research on self-assembled monolayers (SAM) of thiols on gold surfaces, the gold-thiol chemistry has been pursued in Au nanoparticle synthesis.[7−9] One of the major goals is to prepare quantum-sized, well-defined gold thiolate nanoclusters.[10−14] A series of distinct gold thiolate clusters, such as the 29 kDa, 22 kDa, 15 kDa, 8 kDa, and ~5 kDa species reported earlier by Whetten and co-workers,[6,28−30] have started to be unraveled with respect to their molecular formula as well as crystal structures. Among them, the 5 kDa species (initially assigned $Au_{28}(SR)_{16}$ clusters[28,29] has been determined to be $Au_{25}(SR)_{18}$ clusters.[10,31] By running high resolution electrophoresis, Tsukuda and co-workers isolated a number of size discrete $Au_n(SG)_m$ species and determined their sizes by electrospray ionization (ESI) mass spectrometry.[10] In their early work, Murray and co-workers and Quinn *et al.*,[32,33] reported the synthesis and electrochemical properties of $Au_{\sim 140}$ and $Au_{38}(SR)_{24}$ clusters (the latter has been corrected as $Au_{25}(SR)_{18}$ clusters[34]). We have recently reported a high yielding method for synthesizing $Au_{25}(SR)_{18}$ clusters *via* kinetic control.[11,35,36] This approach has also been extended to the synthesis of $Au_{20}(SR)_{16}$ clusters.[37] The chiroptical properties of Au_n thiolate clusters have been extensively investigated by Yao and Burgi and their respective co-workers[38,39] since the initial work by Whetten *et al.*[29]

Recently, Jadzinsky *et al.* reported the crystal structure of a $Au_{102}(SPhCOOH)_{44}$ nanocluster.[40] The $Au_{102}(SR)_{44}$ cluster should be relevant to the 22 kDa species. A second gold thiolate cluster structure is $[Au_{25}(SC_2H_4Ph)_{18}]^-TOA^+$, independently reported by Zhu *et al.*[5] and Heaven *et al.*[41] Shortly after that, Zhu *et al.* also succeeded in crystallization of an air-oxidized product of the $[Au_{25}(SC_2H_4Ph)_{18}]^-TOA^+$ cluster and this product was determined by X-ray crystallographic analysis to be a charge-neutral 25-atom $[Au_{25}(SC_2H_4Ph)_{18}]^0$ cluster.[42] This neutral cluster possesses an essentially identical structure with the framework of the anionic cluster but with some appreciable differences.[5,42] An interesting aspect of the charge-neutral $[Au_{25}(SC_2H_4Ph)_{18}]^0$ cluster is its intrinsic paramagnetism, which can be reversibly switched on and off by controlling the charge state of the cluster.[43] The observed magnetism of $[Au_{25}(SC_2H_4Ph)_{18}]^0$ was found to originate from an unpaired electron in the highest occupied molecular orbital (HOMO, approximately triply degenerate).[43] The results provide proof that the $Au_{25}(SR)_{18}$ clusters may be viewed as superatoms since they bear some resemblance in the electronic structure with simple atoms.[44]

With respect to the $Au_{38}(SR)_{24}$ cluster, this cluster pertains to the 8 kDa species reported earlier by Schaaff *et al.*,[6,45] but at that time the exact composition was not confirmed by mass spectrometry since the early LDI-MS analysis often resulted in fragmentation of the clusters and thus complicated the cluster composition determination. Recently, Toikkanen *et al.*[46] isolated a relevant species that was determined to be $Au_{38}(SC_6H_{13})_{22}$ by LDI-MS (note: this formula perhaps should be corrected as $Au_{38}(SR)_{24}$). Tsukuda *et al.* reported chromatographic or solvent-extraction isolation and electrospray ionization (ESI) MS determination of $Au_{38}(SC_{12}H_{25})_{24}$ clusters, but the yield was quite low.[47−49] Very recently, Qian *et al.* developed an improved synthetic method and largely improved the $Au_{38}(SC_{12}H_{25})_{24}$ yield (up to ~10%), and the $Au_{38}(SC_{12}H_{25})_{24}$ composition was verified by LDI-MS, ESI-MS, and other characterization.[50]

Despite the substantial effort in synthesizing $Au_{38}(SR)_{24}$ clusters, the mechanistic studies still significantly lag behind. It is certainly of great importance to gain insight into the growth mechanism of $Au_{38}(SR)_{24}$ clusters. Thus far, the best synthetic method for $Au_{38}(SR)_{24}$ in terms of yield and purity seems to be the one reported by Qian *et al.*[50] In this method, a crude mixture of glutathionate-capped $Au_n(SG)_m$ clusters was first made; then, the mixed clusters were subject to a thermal thiol exchange/etching process in a two-phase (water/organic) system. After the $-SG$ to $-SC_{12}H_{25}$ ligand exchange on the $Au_n(SG)_m$ clusters is completed, the subsequent etching process (using neat dodecanethiol) causes gold core etching, and eventually the starting polydisperse clusters convert to monodisperse $Au_{38}(SC_{12}H_{25})_{24}$ clusters in high purity. This method eliminates nontrivial postsynthetic separation steps involved in previous work.[49] An important advantage of the improved method is that it can be readily scaled up to synthesize large quantities (*e.g.*, > 0.1 g) of $Au_{38}(SC_{12}H_{25})_{24}$ clusters since the yield was improved to 5−10%.[50]

In this work, we report the synthesis of phenylethylthiolate-capped $Au_{38}(SC_2H_4Ph)_{24}$ clusters with a modified approach on the basis of the previous approach[50] for $Au_{38}(SC_{12}H_{25})_{24}$ and also a preliminary mechanistic study on the growth mechanism of the Au_{38} clusters. Some potentially important factors for the synthesis of Au_{38} clusters have been investigated in details. The synthetic yield of $Au_{38}(SC_2H_4Ph)_{24}$ has been raised to ~25% (Au atom basis). More importantly, mechanistic studies on the conversion process provide important insight into the growth mechanism of $Au_{38}(SC_2H_4Ph)_{24}$ clusters. We found that $Au_{38}(SC_2H_4Ph)_{24}$ clusters are indeed gradually converted from larger clusters in the thiol etching induced growth process. This "size focusing" process is remarkable, and may be extendable to the synthesis of other stable $Au_n(SR)_m$ nanoclusters since the growth process is primarily driven by cluster stability, thus, making the approach of potential broad utility.

RESULT AND DISCUSSION

High Yield Synthesis of Monodisperse $Au_{38}(SC_2H_4Ph)_{24}$ Clusters. In early work, Schaaff *et al.* reported glutathione-protected Au_n clusters.[28] In subsequent research, Negishi *et al.* isolated a series of $Au_n(SG)_m$ clusters by running high resolution polyacrylamide gel electrophoresis (PAGE).[10] The formula of these $Au_n(SG)_m$ clusters (ranging from Au_{10} to Au_{39}) were successfully determined by improved ESI mass spectrometry analysis.[10] It is worth noting that those $Au_n(SG)_m$ clusters were prepared in *methanol* by $NaBH_4$ reduction of polymeric Au(I)−SG complexes. We recently found that the solvent plays a critical role in size control of $Au_n(SG)_m$ clusters.

In regards to the conversion of $Au_n(SG)_m$ to dodecylthiolate-capped $Au_{38}(SC_{12}H_{25})_{24}$ clusters, an important advantage of our previous method is that it solely produces $Au_{38}(SC_{12}H_{25})_{24}$ clusters,[50] instead of a mixture (*i.e.*, Au_{38} and Au_{144}).[49] If a mixture is resulted, the isolation of Au_{38} would be complicated and nontrivial.[49] In our effort to increase the yield of $Au_{38}(SR)_{24}$ clusters, we found that the size distribution of the initial $Au_n(SG)_m$ mixture indeed has a major effect on the final yield of $Au_{38}(SR)_{24}$. Also, we found that the solvent used in the preparation of $Au_n(SG)_m$ mixture affects the size distribution of the $Au_n(SG)_m$ clusters, which subsequently influences the final yield of $Au_{38}(SR)_{24}$ clusters. Motivated by these observations, we have modified the previous synthetic procedure[50] by replacing the reaction solvent (methanol) with other solvents, and found that acetone is a good solvent for high yielding synthesis of $Au_{38}(SR)_{24}$ clusters.

Below we focus on the *acetone*-mediated synthesis of $Au_n(SG)_m$ clusters and conversion into phenylethylthiol-capped $Au_{38}(SC_2H_4Ph)_{24}$ clusters with molecular purity through a size-focusing process. The synthetic method still involves two main steps as the previous protocol, (1) to prepare the starting $Au_n(SG)_m$ clusters in acetone (rather than in methanol), (2) conversion of mixed $Au_n(SG)_m$ clusters into monodisperse Au_{38} clusters *via* thermal etching (Scheme 1). For etching with phenylethylthiol, we found that a 50% (vol) PhC_2H_4SH solution (diluted by toluene) gives rise to the best Au_{38} yield. The reaction of PhC_2H_4SH with the $Au_n(SG)_m$ mixture was conducted in a two-phase system and was allowed to proceed for ~40 h (see Experimental Section for details). Through this improved approach, we have reproducibly obtained $Au_{38}(SC_2H_4Ph)_{24}$ clusters with a significantly improved yield of ~25% (Au atom basis). This is particularly important for future pursuit of their practical applications. Note that the remaining ~75% was lost to Au(I)−SR polymers, which was also identified in our previous work on the synthesis of $Au_{38}(SC_{12}H_{25})_{24}$ clusters.[50] The Au(I)−SR formed from decomposition of $Au_n(SC_2H_4Ph)_m$ cannot be rereduced to clusters to increase the yield.

Scheme 1. A two-step procedure for synthesizing monodisperse $Au_{38}(SC_2H_4Ph)_{24}$ clusters in high yield.

The monodispersity of clusters is a major issue in the synthesis of Au clusters. Herein we employed size exclusion chromatography (SEC) to perform initial characterization on the monodispersity of the as-prepared Au_{38} clusters. A typical SEC chromatogram of Au clusters is shown in Supporting Information Figure S1a (monitored at 630 nm by a diode array detector, DAD). The UV−vis spectra of eluted Au clusters were online recorded by DAD. In the chromatogram (Figure S1), a sharp peak was observed at 14.43 min (fwhm ~0.40 min); the UV−vis spectra at different time points of the peak are perfectly superimposable (Supporting Information Figure S1b), indicating high purity of the clusters.

To further analyze the cluster monodispersity, we employed both MALDI and ESI mass spectrometry to characterize the as-prepared clusters. For MALDI analysis of phenylethylthiolate-capped gold clusters, Dass *et al.* previously reported the observation of *intact* $Au_{25}(SC_2H_4Ph)_{18}$ ions when *trans*-2-[3-(4-*tert*-butylphenyl)-2-methyl-2-propenyldidene] malononitrile (DCTB) was used as the matrix and when the laser pulse intensity was kept low enough (just above the threshold intensity).[51] We followed Dass's method and characterized $Au_{38}(SC_2H_4Ph)_{24}$ clusters by MALDI-TOF. As shown in Figure 1a (top spectrum), a clean MALDI spectrum was observed with an intense peak at ~10780 Da (assigned to the intact $Au_{38}(SC_2H_4Ph)_{24}$ ion, theoretical value: 10778.05 Da). Note that fragmentation still occurs and a peak at ~9342 Da, together with a few others, was found. To confirm these peaks arise from the fragmentation of $Au_{38}(SC_2H_4Ph)_{24}$ clusters rather than being present in the original sample, we investigated the effect of laser pulse intensity on the mass distribution. With decreasing laser intensity (Figure 1a, from top to bottom), the peak at ~9342 Da was found to dramatically decrease relative to the 10780 Da $Au_{38}(SC_2H_4Ph)_{24}$ peak (used as the reference), which means that the 9342 Da peak comes from fragmentation of $Au_{38}(SC_2H_4Ph)_{24}$, otherwise, the relative intensities of the two peaks would be retained. Other small peaks of fragments observed in the mass spectrum are assigned (Supporting Information Figure S2 and Table S1). It is worth noting that a similar fragmentation phe-

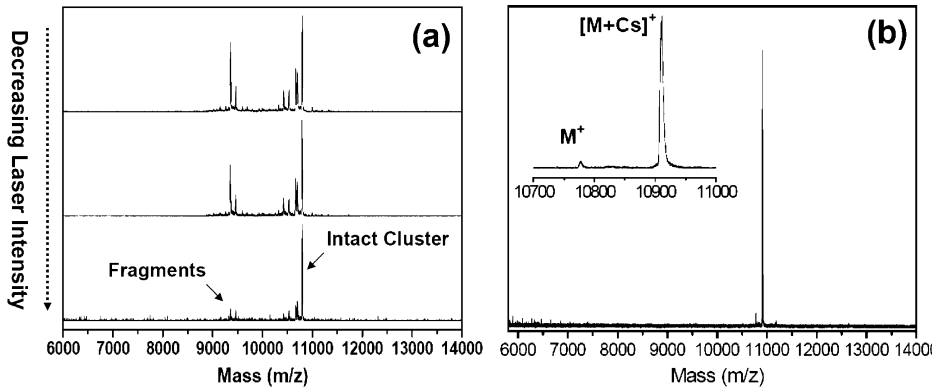

Figure 1. (a) Positive MALDI-TOF mass spectra of $Au_{38}(SC_2H_4Ph)_{24}$ nanoclusters corresponding to different laser intensities (decreasing from top to bottom). (b) ESI mass spectrum of $Au_{38}(SC_2H_4Ph)_{24}$; inset shows the zoomed-in spectrum.

nomenon was observed in the case of MALDI analysis (DCTB as matrix) of $Au_{25}(SC_2H_4Ph)_{18}$: The intact ion of $Au_{25}(SC_2H_4Ph)_{18}$ and its fragment $Au_{21}(SR)_{14}$ were both observed, and the fragmentation becomes more severe under stronger laser intensities. Compared with MALDI, electrospray ionization (ESI) is a much softer ionization technique and typically it can generate mass spectra of unfragmented Au clusters.[49,52,53] Alkali acetate salt (MOAc, M = Na, K, and Cs) was found to enhance cluster ionization by forming adducts of clusters and alkali ions.[52,53] Herein, we use ESI-MS to further characterize the Au_{38} clusters. As shown in Figure 1b, only one intense sharp peak at 10910.69 Da was observed in the ESI spectrum, indicating the high purity of the clusters. The 10910.69 Da peak is assigned to the adduct $[Au_{38}(SC_2H_4Ph)_{24}Cs]^+$ (theoretical value: 10910.95 Da). A small peak at 10777.54 Da is also observed (Figure 1b inset), which corresponds to plain $Au_{38}(SC_2H_4Ph)_{24}$ (ionized form, theoretical value: 10778.05 Da). The absence of any signals at ~9342 Da confirms that the 9342 Da peak observed in the MALDI spectrum arises from a fragment of $Au_{38}(SC_2H_4Ph)_{24}$.

Taken together, both MALDI and ESI results confirm the high purity and the composition of $Au_{38}(SC_2H_4Ph)_{24}$ of the clusters. Thermogravimetric analysis (TGA) of the Au clusters shows a weight loss of 31.2% (Figure S3), very close to the theoretical weight loss (30.5%). On the basis of the TGA result, the ratio of Au-to-ligands can be calculated (*i.e.*, 1.53:1), which is consistent with the theoretical value of Au/SR (38/24 = 1.58, experimental error ~3%).

Molecule-like Optical and Electrochemical Properties of $Au_{38}(SC_2H_4Ph)_{24}$ Clusters. An interesting aspect of $Au_{38}(SC_2H_4Ph)_{24}$ clusters is their molecule-like properties, such as HOMO−LUMO gap and single electron charging.[46,54] These effects are manifested in the optical absorption and electrochemical properties of the clusters.[55]

Figure 2a shows the UV−vis−NIR spectrum of $Au_{38}(SC_2H_4Ph)_{24}$ clusters. A series of peaks appear at 1050 nm (1.18 eV), 750 nm (1.66 eV), 620 nm (2.00 eV), 560 nm (2.21 eV), 520 nm (2.39 eV), and 490 nm (2.53 eV); peaks <400 nm are not included. Among them, the most distinct peak is the one at 2.00 eV, which may serve as a distinct feature of Au_{38}. These peaks are indeed almost identical to those of dodecanethiolate-capped $Au_{38}(SC_{12}H_{25})_{24}$ clusters,[6,48−50] indicating that the optical absorption of the $Au_{38}(SR)_{24}$ clusters is not affected by the tail groups in the thiolate. The optical energy gap is determined to be 0.92 eV by extrapolating the lowest energy absorption peak to zero absorbance (Figure 2a inset), which is close to the previously reported 0.9 eV.[6,49,50]

We have also performed differential pulse voltammetry (DPV) and cyclic voltammetry (CV) analysis of the $Au_{38}(SC_2H_4Ph)_{24}$ clusters (Figure 2b). The first oxidation wave (ox1) and the first reduction wave (re1) lie at +0.48 and −0.71 V (*versus* the quasi-reference Ag electrode), respectively. These values are consistent with the previous electrochemical work on Au_{38} clusters by Quinn *et al.*[46] The CV was shown in supporting Figure S4. The ~1.2 V electrochemical energy gap of $Au_{38}(SC_2H_4Ph)_{24}$ clusters, after subtracting the charging energy (estimated from the difference of ox2 and ox1, *i.e.*, 0.68−0.48 = 0.2 V), converts to the actual HOMO−LUMO gap of 1.0 V for the $Au_{38}(SC_2H_4Ph)_{24}$ cluster, which is close to the optical energy gap (0.92 eV). This HOMO−LUMO gap is smaller than that of $Au_{25}(SR)_{18}$ ($E_g \approx 1.3$ eV),[5] implying a general trend that the larger the clusters are, the smaller is the gap.

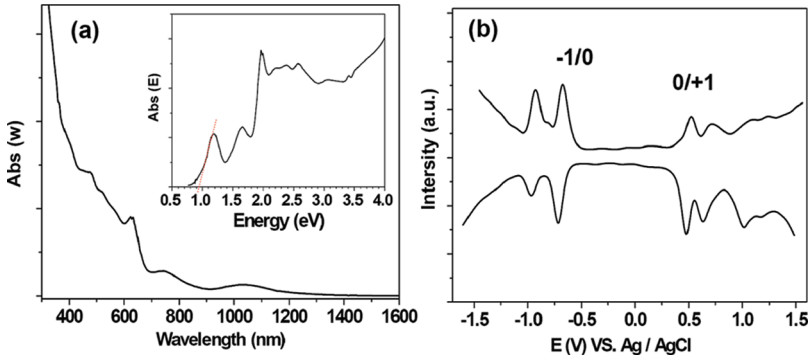

Figure 2. (a) UV−vis spectra of $Au_{38}(SC_2H_4Ph)_{24}$ clusters; the inset shows the spectrum on the energy scale (eV). (b) Differential pulse voltammogram (DPV) at room temperature (measurement conditions: pulse cycle, 0.2 s; scan rate in either direction, 0.05 V/s).

Mechanistic Investigation of the Growth of $Au_{38}(SC_2H_4Ph)_{24}$ Clusters. A major issue is to understand the mechanism of the high yielding growth of monodisperse $Au_{38}(SC_2H_4Ph)_{24}$ clusters. In this work, we further investigated the conversion mechanism. The differ-

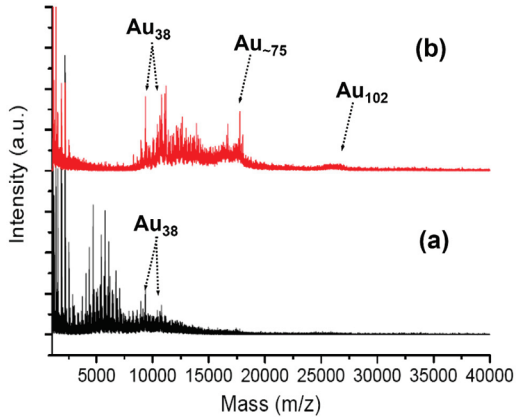

Figure 3. MALDI mass spectra of Au clusters obtained from ligand exchange of $Au_n(SG)_m$ with PhC_2H_4SH (reaction for 10 min). The starting $Au_n(SG)_m$ clusters were made (a) in methanol and (b) in acetone.

ent solvent (acetone *vs* methanol) used for the synthesis of the $Au_n(SG)_m$ mixture has been found to be primarily responsible for the different yields of $Au_{38}(SC_2H_4Ph)_{24}$ clusters in the two syntheses. The $Au_n(SG)_m$ mixture prepared in acetone and methanol may be different in their size distributions. However, it is complicated and time-consuming if one tries to separate each $Au_n(SG)_m$ species and to determine their formula and proportion, as was done by Tsukuda *et al*. in their PAGE work on $Au_n(SG)_m$ clusters.[10] If the $Au_n(SG)_m$ mixture is not separated, the multiply charged anions of each size in the $Au_n(SG)_m$ mixture will lead to very complicated ESI mass spectra that are difficult to analyze. Without attempting to identify the components of the $Au_n(SG)_m$ mixture, we employed MALDI-MS (DCTB as the matrix) to analyze the size distribution of $Au_n(SC_2H_4Ph)_m$ clusters (mixture) that was produced from glutathionate-to-phenylethylthiolate exchange of the starting $Au_n(SG)_m$ clusters. We found that in the two phase system, $-$SG capped Au_n clusters are readily transferred from the water phase to the organic (toluene) phase in less than 10 min in the presence of PhC_2H_4SH. The toluene solution was then sampled for MALDI-MS and UV$-$vis analysis to gain insight into the ligand exchange/etching process. The sample was first purified by wash with methanol to remove excess thiols and then dissolved in CH_2Cl_2 for MALDI-MS and UV$-$vis characterization.

To compare the difference between the $Au_n(SG)_m$ mixture synthesized in different solvents, we have prepared $Au_n(SG)_m$ clusters in methanol and acetone, respectively. For the methanol system, we simply followed the literature method.[10,28,29,50] Previous work by Negishi *et al*. has identified the components of the $Au_n(SG)_m$ mixture (ranging from Au_{10} to Au_{39}). For the phase transferred $Au_n(SC_2H_4Ph)_m$ mixture at the initial stage (reaction time $t = 10$ min), the MALDI mass spectrum (Figure 3a, bottom panel) indeed shows that a range of different sized clusters, the largest cluster being close to ~38 or 39 Au atoms, are present in the $Au_n(SC_2H_4Ph)_m$ mixture, consistent with the previous report.[10] The smaller $Au_n(SG)_m$ clusters ($n < 25$) were previously found to be unstable under thiol etching and decompose to form Au(I)$-$SG.[57] We found that under the harsh conditions (thermal etching with excess thiol at 80 °C), even the relatively robust Au_{25} clusters decompose into Au(I)$-$SR (see Supporting Information, Figure S5). For the starting clusters made in the methanol system, the majority of Au_n clusters are smaller than 38 atoms and were found to decompose into Au(I)$-$SR in our system, thus, limiting the final Au_{38} yield since all these smaller clusters are wasted without converting into Au_{38} clusters. To raise the Au_{38} yield, one needs to prepare relatively larger Au_n clusters with $n > 38$ but not too large, and these size appropriate clusters may convert to Au_{38} by a down-conversion process (*i.e.*, size reduction).

In this work, we modified the previous method[50] for preparing the starting $Au_n(SG)_m$ mixture by replacing methanol with acetone as the reaction solvent. In the acetone system, a significant portion of higher mass clusters was generated, ranging from Au_{38} to $Au_{\sim 75}$, as well as a small portion of Au_{102} (Figure 3b). After thiol etching induced conversion of these starting $Au_n(SG)_m$ clusters, a high yield (~25%) for Au_{38} was attained. We attribute the high yield of $Au_{38}(SC_2H_4Ph)_{24}$ to the down-conversion of those higher mass $Au_n(SG)_m$ clusters ($38 \leq n \leq 102$), that is, these clusters reacted with excess PhC_2H_4SH and were gradually converted to $Au_{38}(SC_2H_4Ph)_{24}$. To provide evidence for that, we investigated the evolution of the reaction mixture by monitoring the UV$-$vis spectrum and MALDI mass spectrum of Au clusters. At different reaction times the solution was sampled for spectroscopic analyses (Figure 4). As aforementioned, the GS$-$ to PhC_2H_4S- thiolate exchange process on $Au_n(SG)_m$ is fast and typically done in ~10 min according to our observation. The similar UV$-$vis spectra of the original $Au_n(SG)_m$ mixture and of the transferred $Au_n(SC_2H_4Ph)_m$ clusters at the initial stage ($t = 10$ min) (Figure 4a) imply that during the initial ~10 min of reaction, the glutathione-capped $Au_n(SG)_m$ clusters are merely transferred from the aqueous solution to the toluene phase with their core sizes essentially unaltered. The size retaining character of thiolate-to-thiolate exchange is in contrast to the phosphine-to-thiolate exchange[31] in which a size change often occurs.

After the $-$SG to $-SC_2H_4Ph$ thiolate exchange process is complete, the $Au_n(SC_2H_4Ph)_m$ mixture further reacts with excess PhC_2H_4SH at 80 °C; during the period the initial polydisperse $Au_n(SC_2H_4Ph)_m$ clusters gradually convert to a monodisperse product (Au_{38} in our case) over a 40 h period. This size focusing process is explicitly demonstrated in Figure 4a and b. The UV$-$vis spectrum of the initial $Au_n(SC_2H_4Ph)_m$ ($t = 10$ min) shows a decay curve, which typically implies a mixture of Au_n

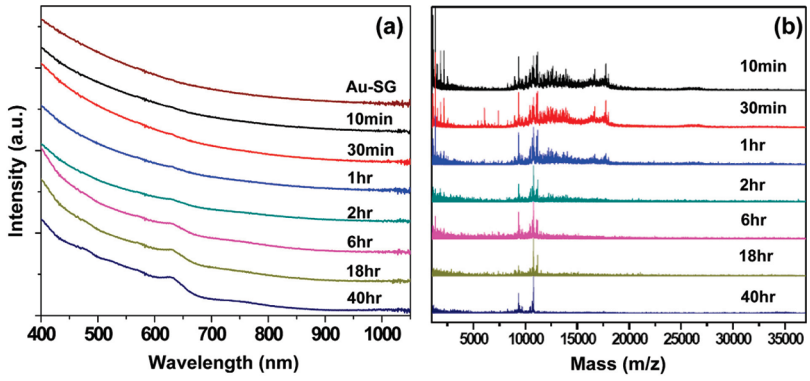

Figure 4. Temporal evolution of UV−vis spectra (a) and MALDI mass spectra (b) of Au clusters during the reaction. Sample Au−SG stands for the $Au_n(SG)_m$ mixture in aqueous solution; 10 min−40 h stands for the time that $Au_n(SG)_m$ ligand exchange/interaction with PhC_2H_4SH.

clusters. As the reaction goes on, the peak at 620 nm and other absorption bands characteristic of $Au_{38}(SR)_{24}$ clusters become distinct. These observations imply that the size distribution of Au_n clusters is gradually "focused" during the thermal thiol-etching process. The corresponding MALDI mass spectra (Figure 4b) provide strong evidence for this remarkable size focusing process of conversion of mixed $Au_n(SC_2H_4Ph)_m$ to monodisperse Au_{38} product. MALDI shows that the initial $Au_n(SC_2H_4Ph)_m$ (t = 10 min) is composed of a mixture of Au clusters ranging from Au_{38} to Au_{102}. With the increase of reaction time, those relative large Au clusters (like Au_{102} and $Au_{\sim 75}$) decompose and convert to Au_{38}. After 2 h of reaction, almost no Au_{102} and $\sim Au_{75}$ were found present in the mixture (Figure 4b). However, Au clusters in the range of $38 \leq Au_n < \sim 75$ were still present with the original Au_{38} clusters. After a longer reaction time (~40 h), only Au_{38} clusters were left in the final solution. The final product shows a distinctive optical spectrum characteristic of Au_{38} clusters (Figure 4a). Note that the 1050 nm absorption peak of Au_{38} clusters is not prominent in the spectra (compare with Figure 2a) due to the insensitivity of Si-based photodiode array detector at wavelength >1000 nm. In the corresponding MALDI spectrum (Figure 4b), an intense mass peak at 10780 Da (assigned to intact $Au_{38}(SC_2H_4Ph)_{24}$ cluster) was observed; note that the peak at 9342 Da is again a fragment of the Au_{38} cluster (see Figure 1). The finally collected Au_{38} clusters show a ~25% yield (Au atom basis).

There are two possible mechanisms for the formation of monodisperse $Au_{38}(SC_2H_4Ph)_{24}$ in relatively high yield. One possibility is that the initial Au_n mixture already contains ~25% Au_{38}, and those larger Au clusters ($38 < n \leq 102$) are merely decomposed into Au(I)−SR. Another possibility is that those larger Au clusters ($38 < n \leq 102$) are etched by excess thiol and the fragments further grow into Au_{38} since Au_{38} seems the most stable cluster in the size range of $38 \leq n \leq 102$ under the current experimental conditions. In the MALDI mass spectrum of the initial $Au_n(SC_2H_4Ph)_m$ (t = 10 min), one indeed finds the existence of Au_{38}; at first glance this might support the first mechanism. However, MS cannot be used for quantitative analysis; therefore, in order to estimate the content of Au_{38} in the initial $Au_n(SC_2H_4Ph)_m$ mixture, we performed size exclusion chromatography analysis of the initial $Au_n(SC_2H_4Ph)_m$ (t = 10 min). The peak area corresponding to Au_{38} is identified by the online-recorded UV−vis spectra. By integrating the area, the proportion of Au_{38} is estimated to be ~ 6%, which is much less than the 25% yield obtained. Therefore, the first mechanism can be ruled out, and it comes to the conclusion that those larger Au_n clusters ($38 < n \leq 102$) should be converted to Au_{38} during the thiol etching-induced growth process.

Overall, these above discussions only provide a "macroscopic" mechanism on the formation of $Au_{38}(SR)_{24}$ from a mixture of $Au_n(SR)_m$ ($38 \leq n \leq 102$). As for the molecular level details on how the etching process occurs and how the fragments or different sized clusters grow into $Au_{38}(SR)_{24}$ clusters, substantial work still needs to be carried out.

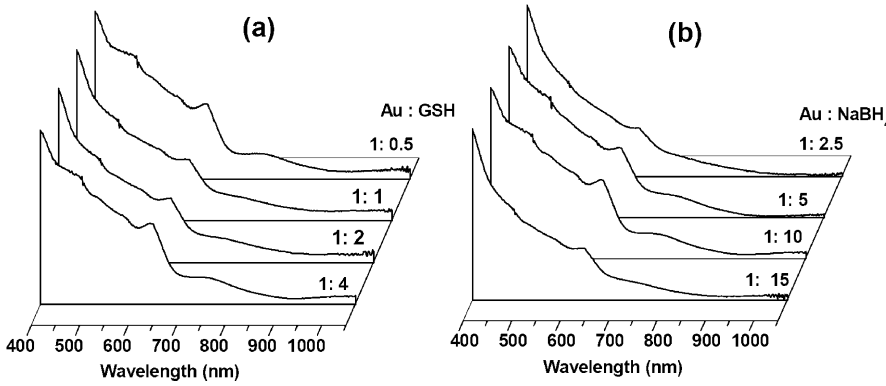

Figure 5. UV−vis spectra of $Au_{38}(SC_2H_4Ph)_{24}$ clusters converted from various $Au_n(SG)_m$ mixtures that were prepared under different conditions: (a) corresponding to $Au_n(SG)_m$ mixtures prepared with different molar ratios of $HAuCl_4$/GSH (the molar ratio of $HAuCl_4$/$NaBH_4$ was fixed at 1:10); (b) corresponding to $Au_n(SG)_m$ mixtures prepared with different molar ratios of $HAuCl_4$/$NaBH_4$ (the molar ratio of $HAuCl_4$/GSH was fixed at 1:4).

Robust Synthesis of $Au_{38}(SC_2H_4Ph)_{24}$ under Various Conditions. Gold cluster synthesis by the modified Brust method[7] is typically quite sensitive to the reaction conditions.[6,30,58] Previously, Murray *et al.* reported that the mean size of Au nanoparticles could be tuned from 1.5 to 5.2 nm by adjusting the Au-to-dodecanethiol ratio, temperature, and reaction rate at which the reduction is conducted.[16] Zhu *et al.* reported a high yielding synthesis of $Au_{25}(SC_2H_4Ph)_{18}$ by kinetic control over the formation of the Au(I)−SR intermediate.[11] All these reports

demonstrate the sensitivity of the Au cluster synthesis to reaction conditions. But we found that Au_{38} clusters can be reproducibly formed under various conditions, that is, quite insensitive to the experimental conditions.

We investigated the reaction conditions such as the ratios of $HAuCl_4$/GSH and of $HAuCl_4$/$NaBH_4$ in the formation of $Au_n(SG)_m$ in acetone. The second thiol etching step was the same as the above protocol. Our results demonstrated that $Au_{38}(SC_2H_4Ph)_{24}$ clusters are reproducibly formed irrespective of the $HAuCl_4$/GSH ratio from 1:0.5 to 1:4, and the ratio of $HAuCl_4$/$NaBH_4$ from 1:2.5 to 1:15, Figure 5. Supporting Information Figures S6 and S7 show the MALDI mass spectra of the initial $Au_n(SC_2H_4Ph)_m$ mixtures obtained from ligand exchange of $Au_n(SG)_m$ mixtures with HSC_2H_4Ph. Under all the reaction conditions investigated, there are more or less Au clusters in the Au_{38} to Au_{102} range (Figure S6 and S7); these clusters are converted into Au_{38} in the thermal thiol etching process, hence, Au_{38} clusters are reproducibly obtained in all the reactions, albeit with different yields. This robust synthesis demonstrates excellent tolerance of our improved synthetic method to the reaction parameters, hence, providing a facile synthetic method for preparing monodisperse $Au_{38}(SC_2H_4Ph)_{24}$ in high yield and on a large scale.

The structure of $Au_{38}(SC_2H_4Ph)_{24}$ remains to be unraveled in future work as crystallization has not been successful thus far, albeit some theoretical work has already predicted the atomic packing structure of this interesting cluster.[59−63] It should be noted that Pei et al. recently predicted a reasonable theoretical structure composed of a face-fused bi-icosahedral core.[63]

CONCLUSION

In summary, we have developed a two-step synthetic method that permits the synthesis of $Au_{38}(SR)_{24}$ clusters in high yield and of molecular purity through conversion of polydisperse $Au_n(SG)_m$ clusters into monodisperse $Au_{38}(SR)_{24}$ in a two phase system. A key modification to our previous approach[50] is to replace the solvent methanol with acetone in the first step of making $Au_n(SG)_m$ clusters. The acetone-mediated synthesis leads to a significant portion of clusters larger than Au_{38} (the main portion is in the range of Au_{38} to $Au_{\sim 102}$). In the subsequent step of thermal thiol etching at 80 °C, these Au_n clusters ($38 < n \leq 102$) are converted to monodisperse $Au_{38}(SR)_{24}$ clusters through a size-focusing process. Our work demonstrates that size-focusing seems an important process in gold cluster synthesis, and monodisperse clusters can be attained by control of the size range of the starting material. Overall, the importance of this work is two-fold: (1) It provides a facile method for high yielding synthesis of Au_{38} in high purity and this method can be readily scaled up for large quantity synthesis. (2) The mechanistic insight into the thiol-etching induced growth process may allow the size-focusing approach to be extended to the synthesis of other robust Au clusters since the process is primarily driven by cluster stability.

EXPERIMENTAL SECTION

Chemicals. Tetrachloroauric(III) acid ($HAuCl_4 \cdot 3H_2O$, 99.99%, Aldrich), 2-phenylethanethiol (PhC_2H_4SH, 99%, Aldrich), glutathione (G-SH, 98%, Acros Organics), sodium borohydride ($NaBH_4$, 99.99%, Aldrich), acetone (HPLC grade, 99.9%, Aldrich), tetrabutylammonium hexafluorophosphate ($TBAPF_6$) (98%, Fluka), toluene (HPLC grade, 99.9%, Aldrich), ethanol (HPLC grade, Aldrich), methanol (HPLC grade, 99%, Aldrich), and dichloromethane (HPLC grade, 99.9%, Aldrich) were used as received.

Synthesis of Monodisperse $Au_{38}(SC_2H_4Ph)_{24}$ Nanoclusters. *Acetone-Mediated Synthesis of Glutathione Protected Au_n Nanoclusters.* In a typical experiment, 0.5 mmol $HAuCl_4 \cdot 3H_2O$ and 2.0 mmol GSH powder were mixed in 20 mL of acetone at room temperature under vigorous stirring for ~20 min. The mixture (yellowish cloudy suspension) was then cooled to ~0 °C in an ice bath. After ~20 min, a solution of $NaBH_4$ (5 mmol, dissolved in 6 mL of cold nanopure water) was rapidly added to the suspension under vigorous stirring. The color of the solution immediately turned black after addition of $NaBH_4$, indicating the formation of Au nanoclusters. After ~20 min, the black $Au_n(SG)_m$ nanoclusters were found to precipitate out and stick to the inner wall of the flask. The clear acetone solution was decanted and 6 mL of water was added to dissolve the $Au_n(SG)_m$ clusters. For the preparation of the $Au_n(SG)_m$ mixture, we have also tested the molar ratios of $HAuCl_4 \cdot 3H_2O$ to GSH (including 1:4, 1:2, 1:1, 1:0.5), and of $HAuCl_4$ to $NaBH_4$ (including 1:15, 1:10, 1:5, 1: 2.5).

The method to prepare $Au_n(SG)_m$ mixture in methanol was reported in our previous work.[50] The solvent (acetone *vs* methanol) was found to greatly affect the $Au_n(SG)_m$ size distribution (*vide infra*).

Conversion of Polydisperse $Au_n(SG)_m$ to Monodisperse $Au_{38}(SC_2H_4Ph)_{24}$ Nanoclusters. Monodisperse $Au_{38}(SC_2H_4Ph)_{24}$ nanoclusters were obtained by reacting $Au_n(SG)_m$ with excess PhC_2H_4SH. Typically, a solution of $Au_n(SG)_m$ (200−300 mg, dissolved in 6 mL of nanopure water) was mixed with 0.3 mL of ethanol, 2 mL of toluene, and 2 mL of PhC_2H_4SH. Here, ethanol is added to prompt the phase transfer of $Au_n(SG)_m$ from water to organic phase. The diphase solution was heated to and maintained at 80 °C under air atmosphere, the $Au_n(SG)_m$ clusters were found to transfer from the water phase to the organic phase in less than 10 min. The thermal process was allowed to continue for ~40 h at 80 °C. Over the long time etching process, the initial polydisperse Au_n nanoclusters were finally converted to monodisperse $Au_{38}(SC_2H_4Ph)_{24}$ clusters. The organic phase was thoroughly washed with ethanol (or methanol) to remove excess thiol. Then the $Au_{38}(SC_2H_4Ph)_{24}$ nanoclusters were simply separated from Au(I)−SG (poorly soluble in almost all solvents) by extraction with dichloromethane or toluene. The yield of Au_{38} nanoclusters was ~25% (Au atom basis), and this yield can be reproducibly obtained.

Characterization. Matrix-assisted laser desorption ionization (MALDI) mass spectrometry was performed with a PerSeptive-Biosystems Voyager DE super-STR time-of-flight (TOF) mass spectrometer. *trans*-2-[3-(4-*tert*-Butylphenyl)-2-methyl-2-propenylidene] malononitrile (DCTB) was used as the matrix for MALDI. Typically, 1 mg of matrix and 0.1 mg of analyte stock solution were mixed in 100 μL of CH_2Cl_2. A 10 μL portion of solution was applied to the steel plate and then air-dried. UV−vis spectra of the Au clusters (dissolved in CH_2Cl_2) were acquired on Hewlett- Packard (HP) Agilent 8453 diode array spectrophotom-

eter and Varian Cary 5000 UV−vis−NIR spectrophotometer at room temperature. Electrospray ionization (ESI) mass spectra were recorded using a Waters Q-TOF mass spectrometer equipped with Z-spray source. The source temperature was kept at 70 °C. The sample was directly infused into the chamber at 5 μL/min. The spray voltage was kept at 2.20 kV and the cone voltage at 60 V. The ESI sample was dissolved in toluene (1 mg/mL) and diluted (1:2 v) by dry methanol (containing 50 mM CsOAc to enhance cluster ionization in ESI). Size exclusion chromatography (SEC, using a PLgel column, particle size of 3 μm, pore diameter of 100 Å) was used to analyze the purity of Au nanoclusters; SEC was performed on a HP Agilent 1100 HPLC system equipped with a diode array detector (DAD). DAD *online* records the UV−vis spectra (190−950 nm range only) of the eluate. The mobile phase was CH_2Cl_2 at a flow rate of 0.5 mL/min. Thermal gravimetric analysis (TGA) (typically ~3 mg sample used) was obtained on a TG/DAT6300 analyzer (Seiko Instruments, Inc.) under a N_2 atmosphere (flow rate ≈ 50 mL/min). Differential pulse voltammetry (DPV) and cyclic voltammogram (CV) measurements of $Au_{38}(SC_2H_4Ph)_{24}$ clusters were performed on a CHI 620C electrochemical station at room temperature under N_2 atmosphere. A platinum wire (the counter-electrode), platinum working electrode, and Ag/Ag^+ quasi-reference electrode were used in the analysis. $Au_{38}(SC_2H_4Ph)_{24}$ solution (~10 mg/mL) was prepared in an electrolyte solution of 0.1 mol/L $TBAPF_6$ in anhydrous CH_2Cl_2, and the solution was bubbled with dry N_2 and blanked under N_2 throughout the electrochemical measurements to minimize O_2 and moisture interference.

Acknowledgment. This work is financially supported by CMU, AFOSR, and NIOSH. We thank Dr. Zhongrui Zhou for assistance in ESI-MS analysis and helpful discussions.

Supporting Information Available: Figures S1−S7, size exclusion chromatogram of as-prepared Au cluster; zoomed-in MALDI spectrum of $Au_{38}(SC_2H_4Ph)_{24}$ clusters and the assignments of the peaks; TGA and cyclic voltammograms of $Au_{38}(SC_2H_4Ph)_{24}$ clusters; size exclusion chromatogram of sample $Au_n(SC_2H_4Ph)_m$ (t = 10 min); MALDI mass spectra of $Au_n(SC_2H_4Ph)_m$ mixtures prepared under different ratio of $HAuCl_4$/GSH and $HAuCl_4/NaBH_4$. This material is available free of charge *via* the Internet at http://pubs.acs.org.

REFERENCES AND NOTES

1. Price, R. C.; Whetten, R. L. Raman Spectroscopy of Benzenethiolates on Nanometer-Scale Gold Clusters. *J. Phys. Chem. B* **2006**, *110*, 22166–22171.
2. Mednikov, E. G.; Dahl, L. F. Nanosized $Pd_{37}(CO)_{28}\{P(p\text{-}Tolyl)_3\}_{12}$ Containing Geometrically Unprecedented Central 23-Atom Interpenetrating Tri-icosahedral Palladium Kernel of Double Icosahedral Units: Its Postulated Metal-Core Evolution and Resulting Stereochemical Implications. *J. Am. Chem. Soc.* **2008**, *130*, 14813–14821.
3. Mondloch, J. E.; Yan, X.; Finke, R. G. Monitoring Supported-Nanocluster Heterogeneous Catalyst Formation: Product and Kinetic Evidence for a 2-Step, Nucleation and Autocatalytic Growth Mechanism of $Pt(0)_n$ Formation from H_2PtCl_6 on Al_2O_3 or TiO_2. *J. Am. Chem. Soc.* **2009**, *131*, 6389–6396.
4. Zhang, Q.; Bu, X.; Zhang, J.; Wu, T.; Feng, P. Chiral Semiconductor Frameworks from Cadmium Sulfide Clusters. *J. Am. Chem. Soc.* **2007**, *129*, 8412–8413.
5. Zhu, M.; Aikens, C. M.; Hollander, F. J.; Schatz, G. C.; Jin, R. Correlating the Crystal Structure of A Thiol-Protected Au_{25} Cluster and Optical Properties. *J. Am. Chem. Soc.* **2008**, *130*, 5883–5885.
6. Schaaff, T. G.; Shafigullin, M. N.; Khoury, J. T.; Vezmar, I.; Whetten, R. L.; Cullen, W. G.; First, P. N.; Gutierrez-Wing, C.; Ascensio, J.; Jose-Yacaman, M. J. Isolation of Smaller Nanocrystal Au Molecules: Robust Quantum Effects in Optical Spectra. *J. Phys. Chem. B* **1997**, *101*, 7885–7891.
7. Brust, M.; Walker, M.; Bethell, D.; Schiffrin, D. J.; Whyman, R. Synthesis of Thiol-Derivatized Gold Nanoparticles in a Two-Phase Liquid−Liquid System. *J. Chem. Soc., Chem. Commun.* **1994**, 801–802.
8. Templeton, A. C.; Wuelfing, W. P.; Murray, R. W. Monolayer-Protected Cluster Molecules. *Acc. Chem. Res.* **2000**, *33*, 27–36.
9. Alvarez, M. M.; Khoury, J. T.; Schaaff, T. G.; Shafigullin, M. N.; Vezmar, I.; Whetten, R. L. Optical Absorption Spectra of Nanocrystal Gold Molecules. *J. Phys. Chem. B* **1997**, *101*, 3706–3712.
10. Negishi, Y.; Nobusada, K.; Tsukuda, T. Glutathione-Protected Gold Clusters Revisited: Bridging the Gap between Gold(I)−Thiolate Complexes and Thiolate-Protected Gold Nanocrystals. *J. Am. Chem. Soc.* **2005**, *127*, 5261–5270.
11. Zhu, M.; Lanni, E.; Garg, N.; Bier, M. E.; Jin, R. Kinetically Controlled, High-Yield Synthesis of Au_{25} Clusters. *J. Am. Chem. Soc.* **2008**, *130*, 1138–1139.
12. Donkers, R. L.; Lee, D.; Murray, R. W. Synthesis and Isolation of the Molecule-like Cluster $Au_{38}(PhCH_2CH_2S)_{24}$. *Langmuir* **2004**, *20*, 1945–1952.
13. Gautier, C.; Burgi, T. Chiral *N*-Isobutyryl-cysteine Protected Gold Nanoparticles: Preparation, Size Selection, and Optical Activity in the UV−vis and Infrared. *J. Am. Chem. Soc.* **2006**, *128*, 11079–11087.
14. Yao, H.; Fukui, T.; Kimura, K. Asymmetric Transformation of Monolayer-Protected Gold Nanoclusters *via* Chiral Phase Transfer. *J. Phys. Chem. C* **2008**, *112*, 16281–16285.
15. Teo, B. K.; Shi, X. B.; Zhang, H. Pure Gold Cluster of 1:9:9:1: 9:9:1 Layered Structure: A Novel 39-Metal-Atom Cluster $[(Ph_3P)_{14}Au_{39}Cl_6]Cl_2$ with an Interstitial Gold Atom in a Hexagonal Antiprismatic Cage. *J. Am. Chem. Soc.* **1992**, *114*, 2743–2745.
16. Hostetler, M. J.; Wingate, J. E.; Zhong, C.-J.; Harris, J. E.; Vachet, R. W.; Clark, M. R.; Londono, J. D.; Green, S. J.; Stokes, J. J.; Wignall, G. D.; *et al*. Alkanethiolate Gold Cluster Molecules with Core Diameters from 1.5 to 5.2 nm: Core and Monolayer Properties as a Function of Core Size. *Langmuir* **1998**, *14*, 17–30.
17. Dass, A. Mass Spectrometric Identification of $Au_{68}(SR)_{34}$ Molecular Gold Nanoclusters with 34-Electron Shell Closing. *J. Am. Chem. Soc.* **2009**, *131*, 11666–11667.
18. Zheng, J.; Petty, J. T.; Dickson, R. M. High Quantum Yield Blue Emission from Water-Soluble Au_8 Nanodots. *J. Am. Chem. Soc.* **2003**, *125*, 7780–7781.
19. Wu, Z.; Gayathri, C.; Gil, R. R.; Jin, R. Probing the Structure and Charge State of Glutathione-Capped $Au_{25}(SG)_{18}$ Clusters by NMR and Mass Spectrometry. *J. Am. Chem. Soc.* **2009**, *131*, 6535–6542.
20. Smith, R. K.; Nanayakkara, S. U.; Woehrle, G. H.; Pearl, T. P.; Blake, M. M.; Hutchison, J. E.; Weiss, P. S. Spectral Diffusion in the Tunneling Spectra of Ligand-Stabilized Undecagold Clusters. *J. Am. Chem. Soc.* **2006**, *128*, 9266–9267.
21. Faraday, M. Experimental Relations of Gold (and other Metals) to Light. *Philos. Trans. R. Soc. London* **1857**, *147*, 145–181.
22. Tsunoyama, H.; Ichikuni, N.; Sakurai, H.; Tsukuda, T. Effect of Electronic Structures of Au Clusters Stabilized by Poly(*N*-vinyl-2-pyrrolidone) on Aerobic Oxidation Catalysis. *J. Am. Chem. Soc.* **2009**, *131*, 7086–7093.
23. Luo, J.; Jones, V. W.; Maye, M. M.; Han, L.; Kariuki, N. N.; Zhong, C.-J. Thermal Activation of Molecularly-Wired Gold Nanoparticles on a Substrate as Catalyst. *J. Am. Chem. Soc.* **2002**, *124*, 13988–13989.
24. Xie, J.; Zheng, Y.; Ying, J. Y. Protein-Directed Synthesis of Highly Fluorescent Gold Nanoclusters. *J. Am. Chem. Soc.* **2009**, *131*, 888–889.
25. Zhou, R. J.; Shi, M. M.; Chen, X. Q.; Wang, M.; Chen, H. Z. Atomically Monodispersed and Fluorescent Sub-Nanometer Gold Clusters Created by Biomolecule-Assisted Etching of Nanometer-Sized Gold Particles and Rods. *Chem.—Eur. J.* **2009**, *15*, 4944–4951.
26. Taylor, K. J.; Pettiette-Hall, C. L.; Cheshnovsky, O.; Smalley, R. E. Ultraviolet Photoelectron Spectra of Coinage Metal Clusters. *J. Chem. Phys.* **1992**, *96*, 3319–3329.
27. Li, J.; Li, X.; Zhai, H. J.; Wang, L. S. Au_{20}: A Tetrahedral Cluster. *Science* **2003**, *299*, 864–867.

28. Schaaff, T. G.; Knight, G.; Shafigullin, M. N.; Borkman, R. F.; Whetten, R. L. Isolation and Selected Properties of a 10.4 kDa Gold: Glutathione Cluster Compound. *J. Phys. Chem. B* **1998**, *102*, 10643–10646.
29. Schaaff, T. G.; Whetten, R. L. Giant Gold-Glutathione Cluster Compounds: Intense Optical Activity in Metal-Based Transitions. *J. Phys. Chem. B* **2000**, *104*, 2630–2641.
30. Alvarez, M. M.; Khoury, J. T.; Schaaff, T. G.; Shafigullin, M.; Vezmar, I.; Whetten, R. L. Critical Sizes in the Growth of Au Clusters. *Chem. Phys. Lett.* **1997**, *266*, 91–98.
31. Shichibu, Y.; Negishi, Y.; Tsukuda, T.; Teranishi, T. Large-Scale Synthesis of Thiolated Au_{25} Clusters *via* Ligand Exchange Reactions of Phosphine-Stabilized Au_{11} Clusters. *J. Am. Chem. Soc.* **2005**, *127*, 13464–13465.
32. Lee, D.; Donkers, R. L.; Wang, G. L.; Harper, A. S.; Murray, R. W. Electrochemistry and Optical Absorbance and Luminescence of Molecule-like Au_{38} Nanoparticles. *J. Am. Chem. Soc.* **2004**, *126*, 6193–6199.
33. Quinn, B. M.; Liljeroth, P.; Ruiz, V.; Laaksonen, T.; Kontturi, K. Electrochemical Resolution of 15 Oxidation States for Monolayer Protected Gold Nanoparticles. *J. Am. Chem. Soc.* **2003**, *125*, 6644–6645.
34. Donkers, R. L.; Lee, D.; Murray, R. W. Synthesis and Isolation of the Molecule-like Cluster $Au_{38}(PhCH_2CH_2S)_{24}$. *Langmuir* **2008**, *24*, 5976.
35. Wu, Z.; Jin, R. Stability of the Two Au-S Binding Modes in $Au_{25}(SG)_{18}$ Nanoclusters Probed by NMR and Optical Spectroscopy. *ACS Nano* **2009**, *3*, 2036–2042.
36. Wu, Z.; Suhan, J.; Jin, R. One-Pot Synthesis of Atomically Monodisperse, Thiol-Functionalized Au_{25} Nanoclusters. *J. Mater. Chem.* **2009**, *19*, 622–626.
37. Zhu, M.; Qian, H.; Jin, R. Thiolate-Protected Au_{20} Clusters with a Large Energy Gap of 2.1 eV. *J. Am. Chem. Soc.* **2009**, *131*, 7220–7221.
38. Yao, H.; Miki, K.; Nishida, N.; Sasaki, A.; Kimura, K. Large Optical Activity of Gold Nanocluster Enantiomers Induced by a Pair of Optically Active Penicillamines. *J. Am. Chem. Soc.* **2005**, *127*, 15536–15543.
39. Gautier, C.; Burgi, T. Chiral Inversion of Gold Nanoparticles. *J. Am. Chem. Soc.* **2008**, *130*, 7077–7084.
40. Jadzinsky, P. D.; Calero, G.; Ackerson, C. J.; Bushnell, D. A.; Kornberg, R. D. Structure of a Thiol Monolayer-Protected Gold Nanoparticle at 1.1 Å Resolution. *Science* **2007**, *318*, 430–433.
41. Heaven, M. W.; Dass, A.; White, P. S.; Holt, K. M.; Murray, R. W. Crystal Structure of the Gold Nanoparticle $[N(C_8H_{17})_4][Au_{25}(SCH_2CH_2Ph)_{18}]$. *J. Am. Chem. Soc.* **2008**, *130*, 3754–3755.
42. Zhu, M.; Eckenhoff, W. T.; Pintauer, T.; Jin, R. Conversion of Anionic $[Au_{25}(SCH_2CH_2Ph)_{18}]^-$ Cluster to Charge Neutral Cluster *via* Air Oxidation. *J. Phys. Chem. C* **2008**, *112*, 14221–14224.
43. Zhu, M.; Aikens, C. M.; Hendrich, M. P.; Gupta, R.; Qian, H.; Schatz, G. C.; Jin, R. Reversible Switching of Magnetism in Thiolate-Protected Au_{25} Superatoms. *J. Am. Chem. Soc.* **2009**, *131*, 2490–2492.
44. Walter, M.; Akola, J.; Lopez-Acevedo, O.; Jadzinsky, P. D.; Calero, G.; Ackerson, C. J.; Whetten, R. L.; Gronbeck, H.; Hakkinen, H. A Unified View of Ligand-Protected Gold Clusters as Superatom Complexes. *Proc. Natl. Acad. Sci. U.S.A.* **2008**, *105*, 9157–9162.
45. Schaaff, T. G.; Whetten, R. L. Controlled Etching of Au:SR Cluster Compounds. *J. Phys. Chem. B* **1999**, *103*, 9394–9396.
46. Toikkanen, O.; Ruiz, V.; Ronholm, G.; Kalkkinen, N.; Liljeroth, P.; Quinn, B. M. Synthesis and Stability of Monolayer-Protected Au_{38} Clusters. *J. Am. Chem. Soc.* **2008**, *130*, 11049–11055.
47. Tsunoyama, H.; Negishi, Y.; Tsukuda, T. Chromatographic Isolation of "Missing" Au_{55} Clusters Protected by Alkanethiolates. *J. Am. Chem. Soc.* **2006**, *128*, 6036–6037.
48. Tsunoyama, H.; Nickut, P.; Negishi, Y.; Al-Shamery, K.; Matsumoto, Y.; Tsukuda, T. Formation of Alkanethiolate-Protected Gold Clusters with Unprecedented Core Sizes in the Thiolation of Polymer-Stabilized Gold Clusters. *J. Phys. Chem. C* **2007**, *111*, 4153–4158.
49. Chaki, N. K.; Negishi, Y.; Tsunoyama, H.; Shichibu, Y.; Tsukuda, T. Ubiquitous 8 and 29 kDa Gold:Alkanethiolate Cluster Compounds: Mass-Spectrometric Determination of Molecular Formulas and Structural Implications. *J. Am. Chem. Soc.* **2008**, *130*, 8608–8610.
50. Qian, H.; Zhu, M.; Andersen, U. N.; Jin, R. Facile, Large-Scale Synthesis of Dodecanethiol-Stabilized Au_{38} Clusters. *J. Phys. Chem. A* **2009**, *113*, 4281–4284.
51. Dass, A.; Stevenson, A.; Dubay, G. R.; Tracy, J. B.; Murray, R. W. Nanoparticle MALDI-TOF Mass Spectrometry without Fragmentation: $Au_{25}(SCH_2CH_2Ph)_{18}$ and Mixed Monolayer $Au_{25}(SCH_2CH_2Ph)_{18-x}(L)_x$. *J. Am. Chem. Soc.* **2008**, *130*, 5940–5946.
52. Tracy, J. B.; Crowe, M. C.; Parker, J. F.; Hampe, O.; Fields-Zinna, C. A.; Dass, A.; Murray, R. W. Electrospray Ionization Mass Spectrometry of Uniform and Mixed Monolayer Nanoparticles: $Au_{25}[S(CH_2)_2Ph]_{18}$ and $Au_{25}[S(CH_2)_2Ph]_{18-x}(SR)_x$. *J. Am. Chem. Soc.* **2007**, *129*, 16209–16215.
53. Qian, H.; Jin, R. Controlling Nanoparticles with Atomic Precision: The Case of $Au_{144}(SCH_2CH_2Ph)_{60}$. Nano Lett. Published online September 9, 2009. http://pubs.acs.org/doi/full/10.1021/nl902300y.
54. Chen, S. W.; Ingram, R. S.; Hostetler, M. J.; Pietron, J. J.; Murray, R. W.; Schaaff, T. G.; Khoury, J. T.; Alvarez, M. M.; Whetten, R. L. Gold Nanoelectrodes of Varied Size: Transition to Molecule-Like Charging. *Science* **1998**, *280*, 2098–2101.
55. Murray, R. W. Nanoelectrochemistry: Metal Nanoparticles, Nanoelectrodes, and Nanopores. *Chem. Rev.* **2008**, *108*, 2688–2720.
56. Shibu, E. S.; Muhammed, M. A. H.; Tsukuda, T.; Pradeep, T. Ligand Exchange of $Au_{25}SG_{18}$ Leading to Functionalized Gold Clusters: Spectroscopy, Kinetics, and Luminescence. *J. Phys. Chem. C* **2008**, *112*, 12168–12176.
57. Shichibu, Y.; Negishi, Y.; Tsunoyama, H.; Kanehara, M.; Teranishi, T.; Tsukuda, T. Extremely High Stability of Glutathionate-Protected Au_{25} Clusters Against Core Etching. *Small* **2007**, *3*, 835–839.
58. Whetten, R. L.; Khoury, J. T.; Alvarez, M. M.; Murthy, S.; Vezmar, I.; Wang, Z. L.; Stephens, P. W.; Cleveland, C. L.; Luedtke, W. D.; Landman, U. Nanocrystal Gold Molecules. *Adv. Mater.* **1996**, *8*, 428–433.
59. Hakkinen, H.; Barnett, R. N.; Landman, U. Electronic Structure of Passivated $Au_{38}(SCH_3)_{24}$ Nanocrystal. *Phys. Rev. Lett.* **1999**, *82*, 3264–3267.
60. Hakkinen, H.; Walter, M.; Gronbeck, H. Divide and Protect: Capping Gold Nanoclusters with Molecular Gold-Thiolate Rings. *J. Phys. Chem. B* **2006**, *110*, 9927–9931.
61. Jiang, D.; Tiago, M. L.; Luo, W.; Dai, S. The "Staple" Motif: A Key to Stability of Thiolate-Protected Gold Nanoclusters. *J. Am. Chem. Soc.* **2008**, *130*, 2777–2779.
62. Jiang, D.; Luo, W.; Tiago, M. L.; Dai, S. In Search of a Structural Model for a Thiolate-Protected Au_{38} Cluster. *J. Phys. Chem. C* **2008**, *112*, 13905–13910.
63. Pei, Y.; Gao, Y.; Zeng, X. C. Structural Prediction of Thiolate-Protected Au_{38}: A Face-Fused Bi-icosahedral Au Core. *J. Am. Chem. Soc.* **2008**, *130*, 7830–7832.